Molecular BioSystems

Accepted Manuscript

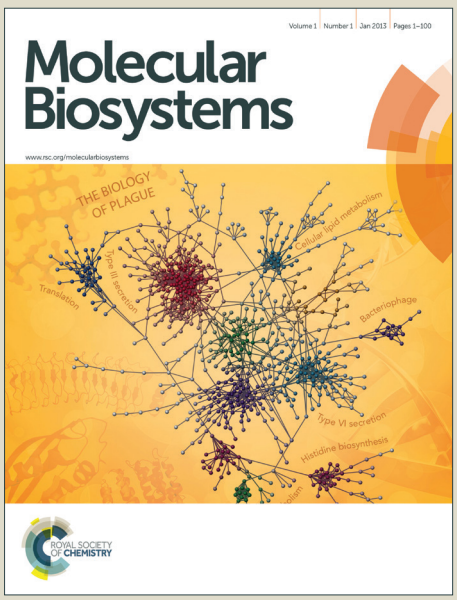

ROYAL SOCIETY OF CHEMISTRY

www.rsc.org/molecularbiosystems

Dynamics matter: Differences and similarities between alternatively designed mechanisms

Ahmet Ay
Departments of Biology and Mathematics, Colgate University
13 Oak Drive, Hamilton, NY 13346

Necmettin Yildirim*
Division of Natural Sciences, New College of Florida
5800 Bayshore Road, Sarasota, FL 34243

April 29, 2014

Abstract

Cells selectively respond to external stimuli to maintain cellular homeostasis by making use of different regulatory mechanisms. We studied two classes of signal-dependent regulatory inhibition and activation mechanisms in this study. Inhibition mechanisms assume that inhibition can occur in two different ways: either by increasing the degradation rate or decreasing the production rate. Similarly, it is assumed that signal-triggered activation can occur either through increasing production rate or decreasing degradation rate. We devised mathematical models (deterministic and stochastic) to compare and contrast responses of these activation and inhibition mechanisms to a time dependent discrete signal. Our simulation results show that the signal-dependent increased degradation mechanism is a more effective, noisier and quicker way to inhibit the protein abundance compared to the signal-dependent decreased activation mechanism. On the other hand, the signal-dependent increased production mechanism can produce a much stronger and faster response than the signal-dependent decreased degradation mechanism. However, our simulations predict that both of the

*Corresponding author: E-mail addresses: nyildirim@ncf.edu, tel: (941) 487-4214; fax: (941) 487-4396;

activation mechanisms have roughly similar noise structures. Our analysis exemplifies the importance of mathematical modeling in the analysis of biological regulatory networks.

Keywords: Mathematical modeling, numerical simulation, stochastic simulation, signal transduction, gene regulatory network

1 Introduction

To maintain cellular homeostasis in response to changes in intracellular and environmental conditions, a cell must be able to regulate its internal network of processes and macromolecules. Such regulation can occur at multiple levels, from genes to proteins along with the intermediate processes and components that link them. At the gene level, the cell can employ various mechanisms to regulate transcription, allowing for control over the production of mRNA [9]. In turn, mRNA can be regulated through RNA processing or degradation [38, 22]. Furthermore, the cell can regulate translation in order to control the direct production of proteins [10, 44]. The resulting proteins can further be regulated through protein folding, reversible and irreversible covalent modifications, translocation, or degradation [26, 30, 3]. These basic mechanisms are used by cells to achieve distinct physiological effects, which may include activation or inhibition of specific cellular functions. Separately, each mechanism offers a distinct regulatory effect; however, it is the combination of basic mechanisms that contributes to the complexity and size of the cellular regulatory network that maintains cellular fitness and versatility.

A common goal in systems biology is to understand the complete cellular regulatory network and the principles that govern the interactions between genes, proteins and other signaling molecules. Since, mechanistic analysis of the complete regulatory network is often overwhelmingly difficult, most of the existing research has focused on small-scale regulatory sub-networks. These studies have successfully uncovered conserved regulatory motifs in the complete network and determined the distinct behaviors each motif confers upon the cell. The transcriptional and the other regulatory motifs include feed-forward loops, autoregulation, negative-feedback loops, to name a few [41, 1, 52, 36]. These motifs utilize the basic control mechanisms to generate biologically important dynamic behaviors, such as oscillations, generation of molecular pulses, and rapid or delayed responses [1, 2, 42, 53, 36]. While certain multiple regulatory architectures may elicit qualitatively similar dynamics, such as oscillations, differences in network architecture may result in distinct properties that are physiologically important to maintain cellular homeostasis [29, 24, 1, 5]. Comparing different network architectures will help reveal their distinct physiological properties to

elucidate the biological roles and importance of the regulatory network architecture.
Here we present two sets of alternatively structured regulatory mechanisms to study their distinct behavioral effects. We define a system centered on a protein P, whose abundance depends on the dynamics between its production and degradation rates. We stimulate the system with a transient signal, which may positively or negatively affect the synthesis or degradation rate of the protein. In studying how changes in signal amplitude and persistency affect the temporal changes in the protein level measured by four response metrics characterizing different aspects of the protein dynamics. We aim to determine the mechanistic properties specific to each mechanism's architecture. As response metrics, we use maximum/minimum protein abundance (mP), time required for the protein to reach 90% of its maximum/minimum abundance (mT), duration of response (D) and integrated response (IR). Such metrics are depicted in Figure 1. D is defined as the total time for which the protein (P) levels are below (for inhibition mechanisms) or above (for activation mechanisms) 10% of its steady state level. IR is the relative increase or decrease of the target protein's effect to downstream targets throughout time, which is measured as the sum of the reduction (for inhibition mechanisms) or increase (for activation mechanisms) of the protein (P) levels throughout time. By using such metrics, we compare the response of alternatively designed inhibition and activation mechanisms to an external stimulus. The results of this study provide further insights into the dynamic regulation of proteins that plays crucial roles in cellular functions in living organisms.
======= Figure 1 here ======================

2 Mathematical Models

The mathematical models presented in this study describe four different mechanisms depicted in Scheme 1 in regulating a generic protein (P) through a transient signal $S(t)$. To study dynamic responses of these similar biological regulatory mechanisms, we devised simple ordinary differential equation (ODE) models according to mass-action kinetics. Although the models differ in their exact mechanisms and equations, they utilize common parameters. In all the models, the net rate of change in the protein abundance ($\frac{dP}{dt}$) is assumed to be the difference between its production and degradation rates and can be written as in Eq.(1).

$$\frac{dP}{dt} = \alpha - \beta P \tag{1}$$

In this equation, the production rate is assumed to be constant (α) and the degradation

rate (βP) is assumed to be a linear function of the protein abundance. To explore the signal dependent responses of the simple regulatory activation mechanisms, we multiply the production rate α by $1 + S(t)$ to increase production or divide the degradation rate βP by $1 + S(t)$ to decrease degradation. Similarly, to study the simple regulatory inhibition mechanisms, we divide the rate of production α by $1 + S(t)$ or multiply the rate of degradation βP by $1 + S(t)$.

======= Scheme 1 here ==========

For example, in order to obtain two different signal-induced inhibition mechanisms, the degradation rate β can be multiplied by $1 + S(t)$ (increased degradation rate as in M_1 in Scheme 1), which results in Eq.(2)

$$\frac{dP}{dt} = \alpha - \beta(1 + S(t))P \tag{2}$$

or the production rate α can be divided by $1 + S(t)$ (decreased production rate as in M_2 in Scheme 1), which leads to Eq.(3).

$$\frac{dP}{dt} = \frac{\alpha}{1 + S(t)} - \beta P \tag{3}$$

It is important to note that in the absence of the signal, all of the models include a constant formation rate and a linear degradation rate, which yield a nonzero steady state protein abundance at $P^* = \alpha/\beta$.

The time dependent signal profile $S(t)$ above is assumed to be a step function with two parameters γ and k, and it has the following form

$$S(t) = \begin{cases} \gamma\,, & \text{if } \ 0 \le t < k \\ 0\,, & \text{if } \ t \ge k \end{cases} \tag{4}$$

The signal amplitude parameter (γ) measures the system's sensitivity to the perturbation caused by the signal. The signal persistency parameter (k) controls how long the signal is applied to the system.

2.1 Inhibition Mechanisms

The first set of mechanisms are governed by the following two differential equations in Eqs.(5) and (6)

$$\frac{dP_1}{dt} = \alpha - \beta\left(1 + S(t)\right)P_1 \quad (5)$$

$$\frac{dP_2}{dt} = \frac{\alpha}{1 + S\left(t\right)} - \beta P_2 \quad (6)$$

The parameter α is the basal rate of the protein formation, which combines transcriptional, post-transcriptional and translational rates. The parameter β represents the degradation rate, which includes regulatory steps such as irreversible post-translational modifications and degradation. These equations model two distinct mechanisms of signal-induced transient inhibition of the protein. The first model given by Eq.(5) describes a signal mediated increase in the protein degradation rate, while the second model given by Eq.(6) represents a signal dependent decrease in the protein formation rate. Eq.(5) maintains the basal formation rate, α, and also includes a degradation rate, β, which is regulated by the signal $S(t)$. Eq.(6) maintains the basal degradation rate, β, and also includes a formation rate α, that is decreased by the signal $S(t)$.

2.2 Activation Mechanisms

The following two equations model two different regulatory mechanisms of a signal induced transient activation of the protein abundance.

$$\frac{dP_3}{dt} = \alpha - \beta\left(\frac{1}{1 + S(t)}\right)P_3 \quad (7)$$

$$\frac{dP_4}{dt} = \alpha\left(1 + S\left(t\right)\right) - \beta P_4 \quad (8)$$

In the first mechanism, the transient increase in the protein level is due to a signal-induced decrease in the protein degradation rate, which is modeled by Eq.(7). In the second mechanism, we assume that the increase in the protein abundance is due to an increase in its formation rate, which is modeled by Eq.(8). The model in Eq.(7) includes the basal formation rate, α, along with a degradation rate, β, which is negatively regulated by the signal $S(t)$. Eq.(8) maintains the basal degradation rate, β, and includes the protein formation rate, α, that is positively regulated by the signal $S(t)$.

2.3 Parameter Values

In this section, we detail how the model parameter values are collected from the literature for *E.coli*

- β: The protein half life changes from protein to protein and varies from 15 to 120 minutes in *E.coli* [49]. Assuming the degradation occurs exponentially, these figures give two estimates of 0.0462 and 0.0057 min^{-1} for the degradation rate β. In this study, we used 0.02 min^{-1} for this parameter, which is approximately equal to the average of these two numbers and indicates a half life of 35 minutes for the protein.

- α : The protein production rate α is estimated as 10-150 molecules/minute in *E.coli* [28]. Ishihama et al. [20] experimentally studied the protein abundances in *E.coli* and classified all proteins in *E.coli* into three groups and reported that the average protein molecule number per gene as 500 molecules. In this study, we took protein production rate α as 10 molecules/minute in the absence of the signal, which results in the steady state of the protein abundance as $P^* = \alpha/\beta = 10/0.02 = 500$ molecules/cell.

- k : This parameter is used to mimic the signal persistency that is observed in signal transduction pathways. Smaller values of this parameter mimic a less persistent signal whereas larger values of this parameter represent a more persistent signal. The value of this parameter changes between 5 to 100 minutes for deterministic simulations. To study the effect of the signal to noise dynamics, we used a more persistent signal with $k = 200$ minutes in the stochastic simulations.

- γ : This parameter refers to the system's sensitivity to the signal. We varied this parameter between 0 to 19, resulting in up to a 20 fold change in the production/degradation rates in the deterministic simulations. For the stochastic simulation, we fixed this parameter at $\gamma = 2$.

2.4 The Solutions of the Models

In this section, we give the analytical solutions of the models in Eqs.(5)-(8) for all of the mechanisms with two different initial conditions: (i) $P_j(0) = \frac{\alpha}{\beta}$ for $0 \leq t < k$ and (ii) $P_j(k) = A_j$ for $k \leq t \leq 600$ for $j = 1, 2, 3, 4$. The solutions are provided in Table 1. The details of the steps of these solutions are given in the supplementary materials. Here A_j s are the protein levels when the signal is removed.

======== Table 1 HERE ========

3 Results

In sections 3.1 and 3.2, we summarize how the response metrics change as the signal amplitude γ and the signal persistency k change in the deterministic models. In Section 3.3, the results of our stochastic simulation will be summarized. We will discuss the dependency of our results to the initial protein abundance determined by the parameters α and β in Section 3.4.

3.1 Comparison of the Inhibition Mechanisms

In both mechanisms M_1 (increase in the degradation rate) and M_2 (decrease in the production rate), the signals diminish protein abundance, but they employ distinct biological mechanisms. Our simulations show that increasing the degradation rate (mechanism M_1) is more effective in diminishing the amount of protein than decreasing the formation rate (mechanism M_2) (Figure 2A). As a response to a 20 fold increase in the signal amplitude with a persistent signal (k is large), the minimum amount of the protein level (mP) decreases down to 24 molecules/cell in mechanism M_1 as opposed to 89 molecules/cell in mechanism M_2. This suggests a $\sim$3.7 fold difference in minimum protein mP values between the two mechanisms for this signal profile. Since our models assume constant production and linear degradation rates for the protein, decreasing the production rate diminishes the production of the protein linearly while increasing the degradation rate exponentially decreases the production over time. This explains the $\sim$3.7 fold difference between the two mechanisms in our simulations. In mechanism M_1, when signal amplitude γ is greater than a threshold value ($\sim$10 fold increase) the signal persistency k has much smaller effect on mP levels. For smaller signal amplitude, the signal persistency alone can still decrease protein level to $\sim$100 molecules/cell. This observation suggests that a persistent signal in mechanism M_1, but not in M_2, can have a significant role in regulating the protein level even for the signal profiles with small amplitude. Unlike what has been observed in mechanism M_1, a persistent signal is required to significantly decrease the protein levels in mechanism M_2. Furthermore, dependency of mP levels on the signal persistency k and amplitude γ parameters in mechanisms M_1 and M_2 is quite different. For a fixed value of signal persistency, mechanism M_1 has more variation in comparison to mechanism M_2. However, for any fixed value of the signal amplitude $\gamma \geq 7$, the opposite behavior is observed. This suggests that while varying signal amplitude leads to higher variation in protein abundance in mechanism M_1, similar behavior can be obtained in mechanism M_2 by varying the signal persistency parameter.

======= Figure 2 here ==========

Interestingly, the M_1 and M_2 mechanisms display different behaviors with regards to time required to reach minimum protein levels(mT) (Figure 2B). Given the same signal profile, increasing the degradation rate(mechanism M_1) produces a quicker response, whereas decreasing the production rate(mechanism M_2) leads to a gradual response. Since the persistent signal causes more severe responses in both mechanisms, the time required to reach the minimum protein level(mT) increases as the signal persistency increases. On the other hand, mechanisms M_1 and M_2 show very distinct mT dynamics with respect to γ and k. For a fixed signal persistency, while we observe roughly the same mT for any signal amplitude in mechanism M_2, there is a nonlinear dependence of mT on the signal amplitude in mechanism M_1. In mechanism M_1, for a fixed signal persistency k, as the signal amplitude increases the mT levels decrease.

Our simulations also show that the M_1 and M_2 mechanisms exhibit similar behavior in the duration metric D, the time period on which the protein levels are reduced by more than 10% of the steady state value (Figure 2C). However, they display different behavior on the integrated response metric IR, the combined effect of the signal to the target proteins (Figure 2D). We observed that, for both of the mechanisms, duration D is independent from the signal amplitude for a fixed value of signal persistency and it stays unchanged as γ varies (Figure 2C). Mechanism M_1 produces a larger integrated response in comparison to mechanism M_2. This difference can be explained as the combined effect of the signal yielding a smaller mP in mechanism M_1 and a roughly similar D in both M_1 and M_2 mechanisms. The numerical simulations reveal that mechanism M_2 shows a constant-like IR dynamics in comparison to mechanism M_1 for a fixed value of signal persistency. For a fixed value of k , the integrated response IR is independent from the signal amplitude when signal amplitude γ is greater than 5 in mechanism M_2 and greater than 15 in mechanism M_1 (Figure 2D).

Although these two different mechanisms have the same general regulatory behavior (decrease in protein levels), cells selectively use these regulatory mechanisms as needed. The systems that require an urgent and severe response would be better off using the degradation mechanism (M_1), which has a more direct effect on the protein than a production mechanism (M_2). Mechanism M_2 may be more practical in regulating the protein levels in systems that need long-term responses or whose effects need not be immediate after the signal. A few examples of biological systems that include an integral degradation mechanism are the cell cycle control (p53), canonical Wnt and NF-kB signaling networks. In the first system, the ubiquitin ligase activity of Mdm2 ubiquitinates p53, facilitating the association of p53 with the proteosome leading to degradation of p53. The increased degradation can

be attributed to the feedback loop involving p53 and Mdm2. The onset of DNA damage first results in decreased p53 degradation; however, p53 enhances the expression of Mdm2, which ultimately leads to an increase in degradation, accounting for the short-term spike in p53 activity. This is a more complicated mechanism, but the increase in the degradation rate of p53 is important since it maintains p53 levels in balance, with short deviations from basal conditions [14, 33, 25]. In the canonical Wnt pathway, the binding of Wnt-5a inhibits the pathway via the GSK-3-independent degradation of beta-catenin, an integral component of the canonical pathway [50]. In the NF-kB pathway, the binding of a ligand such as TNF-alpha activates the pathway, leads to increased IkK activity, which phosphorylates IkB, an inhibitor of NF-kB that controls its translocation into the nucleus. Phosphorylation of IkB leads to further ubiquitination of two lysine residues, targeting the compound for proteosomal degradation [4, 37].

The M_2 mechanism can also be found within the p53, canonical Wnt and NF-kB signaling networks. Upon activation of the p53 pathway in response to DNA damage, p53, being a transcription factor, suppresses myc expression to promote G1 arrest, while also suppressing the expression of cyclin B1 to prevent the cell from moving into the G2 phase [19, 17]. In the canonical Wnt pathway, the translocation of beta-catenin, a transcription factor, represses the expression of Sox9 [8, 16, 51]. In the NF-kB pathway, activation and translocation of NF-kB results in the transcriptional repression of c-myc and Sox9 [35].

Mechanisms M_1 and M_2 can coexist in the same biological systems. However, the systems can employ them in different parts of the network depending on cellular needs.

3.2 Comparison of the Activation Mechanisms

Both mechanisms M_3 (decrease in the degradation rate) and M_4 (increase in the production rate) promote protein (P) levels in the cell through distinct biological mechanisms. Our simulations predict that increasing the production rate (mechanism M_4) seems to be more effective in significantly increasing the maximum levels of the protein (mP) (Figure 3A). For persistent and high amplitude signal ($\gamma = 20$ and $k = 100$), while in mechanism M_3 protein level can go up to 1280 molecules/cell($\sim$2.6 fold of the steady state level) , in mechanism M_4 it can increase up to 8315 molecules/cell ($\sim$16.6 fold of the steady state level). This suggests that mechanism M_4 can increase mP levels $\sim$6.5 fold more than mechanism M_3. Moreover, mP dependency on the signal persistency and the signal amplitude in mechanisms M_3 and M_4 is significantly different. Similarly, for a fixed value of signal persistency, mechanism M_3 has less variation in comparison to mechanism M_4. However, for a fixed value of the signal amplitude, the opposite behavior is observed. This suggests that while

varying signal amplitude leads to a higher variation in protein abundance in mechanism M_4, similar behavior can be obtained in mechanism M_3 by varying the signal persistency.
======= Figure 3 here ==========

Interestingly, M_3 and M_4 mechanisms show similar dynamics in the mT metric (time needed for the protein to reach its maximum level) as the signal persistency and signal amplitude change (Figure 3B). Despite a qualitative similarity, M_4 mechanism shows a slightly faster response. In both mechanisms M_3 and M_4, for fixed signal persistency, mT does not change as signal amplitude γ varies. However, for both mechanisms, when signal amplitude γ is held constant, mT value increases as the signal persistency k increases. This can be explained by the fact that the persistent signal pushes the system to a higher mP abundance in the later time points. Our simulations show that M_3 and M_4 mechanisms exhibit similar qualitative and quantitative behaviors on the duration D metric (Figure 3C). Similar dynamics in mT has been observed for D. However, these two mechanisms display different behavior in the integrated response metric IR (Figure 3D). Mechanism M_4 provides a larger integrated response IR in comparison to mechanism M_3 since M_4 has a similar duration metric D but larger mP. Regarding the integrated response metric IR, mechanisms M_3 and M_4 show different IR dynamics as a response to the changes in the signal persistency and signal amplitude. The numerical simulations reveal that mechanism M_3 shows a more constant-like behavior than mechanism M_4 for a fixed signal persistency.

Biological organisms optimize the regulatory mechanisms they employ in different parts of the cell depending on their needs. They are capable of producing an appropriate response to external signals in a timely fashion. Our simulations show that the protein levels are higher in mechanism M_4 in comparison to mechanism M_3 for the same amount of signal. This observation suggests that a system that needs high level of a certain protein P , the cell should employ mechanism M_4 rather than mechanism M_3. Our simulations also show that the time required to reach maximum protein mP is slightly faster in mechanism M_4. Hence, systems that need short-term response may prefer mechanism M_4, while long-term responses are better suited to mechanism M_3. There is a whole list of other benefits to controlling formation over degradation, one being the multi-level control mechanisms. A system may control transcription, mediators, translation, activation/deactivation, and more. Although there are many mechanisms of degradation, for the most part they all act on the protein itself. A good example of mechanism M_3 can be found in the DNA damage pathway. When p19ARF associates with Mdm2, the latter protein is sequestered, decreasing the likelihood of an interaction between Mdm2 and p53. This interaction eventually leads to p53 activation, and by sequestering Mdm2, the system is reducing the degradation rate of p53 [18, 45, 34]. In the canonical Wnt pathway, activation by a ligand, Wnt, results in the poly-ubiquitination

and phosphorylation of Dishevelled protein, which prevents beta-catenin from the Axin-Gsk3-Ck1a complex that phosphorylates beta-catenin, leading to its eventual ubiquitination and proteosomal degradation. Thus, upon activation of the pathway, the degradation of beta-catenin is decreased, increasing the probability that the protein will reach the nucleus to effect the downstream target genes [23]. In the NF-kB system, ergolide, a sesquiterpene lactone, results in a simultaneous decrease in degradation and reduction in IkK activity, leading to inhibition of the NF-kB pathway (pushes equilibrium towards cytosolic NF-kB-IkB complex) [7].

M_4 mechanism can be observed in the DNA damage pathway. Upon activation of the pathway, free p53 leads to enhanced expression of Mdm2, the ligase responsible for ubiquitinating p53, marking the protein for proteosomal degradation [27, 47, 39, 31, 13, 32]. In the canonical Wnt pathway, beta-catenin directly enhances the expression of cyclin-D [46, 43, 40] and c-myc [15]. In the NF-kB pathway, NF-kB directly enhances the expression of Bcl-2 [6], Bax [12], mouse MHC class I [21] and cyclin-D1 [48].

Mechanisms M_3 and M_4 can coexist in a biological system, which can employ these mechanisms in different parts of the network depending on the needs of the system.

3.3 Stochastic Effects in the Activation and Inhibition Mechanisms

Biological systems are often studied using deterministic methods, where perturbations to system parameters have a predictable and reproducible effect on the system dynamics. However, biochemical reactions in a cell are inherently noisy. The effects of random fluctuations on protein concentrations can be studied by stochastic simulation techniques. Stochastic simulations take random fluctuations in the system into account and capture dynamics that may not be observable by deterministic simulations. To study the possible influence of random fluctuations in the mechanisms M_1, M_2, M_3 and M_4 we have also utilized stochastic simulations. We used the Gillespie Algorithm [11] (implemented in MATLAB) to stochastically simulate the dynamics of all four mechanisms. For each mechanism, five hundred stochastic simulations have been carried out until the system reaches its steady state after the removal of the signal. A relatively small steady state level was selected to investigate effects of noise in the dynamics. In all the stochastic simulations, we fixed the parameter values as $\alpha = 1$, $\beta = 0.02, \gamma = 2$ and $k = 200$, which results in a signal profile with persistency about 200 minutes and a stable steady state of 50 molecules/cell.

Stochastic simulations of the mechanisms M_1 (increased degradation rate) and M_2 (decreased synthesis rate) show different behaviors in terms of noise in earlier time points after the signal has been introduced to the system (Figure 4A). This figure shows the time se-

ries simulation of the protein levels for 600 minutes starting with 50 molecules/cell. For the same signal profile, the mechanism M_1 has more fluctuations than the mechanism M_2 in earlier times (<150 minutes) but not later times (Figure 4). This has been shown by creating the histogram of the protein levels at t=50 minutes (Figure 4B). We calculated the coefficient of variation (CV) for both mechanisms and found CV = 0.24 for mechanism M_1 and CV = 0.14 for mechanism M_2. Therefore, mechanism M_1 exhibits almost two-fold more variation in comparison to mechanism M_2. In later time points, the variation in these two mechanisms are comparable. Such a difference can be explained by a faster response observed in mechanism M_1. This observation is in agreement with our deterministic simulations. At any time before 150 minutes, the number of molecules in M_1 is always smaller than that of in M_2. Due to the small number of molecules at early time points, the stochastic simulations show more variation in mechanism M_1 (Figure 6A). After t = 150 minutes, since both mechanisms converge back to the same steady state levels, they show a similar noise structure.

Similar to mechanisms M_1 and M_2, mechanisms M_3 and M_4 display different behaviors in terms of noise at earlier time points (Figure 5A). For the same signal profile, dynamics in M_4 are noisier than dynamics in M_3 in earlier time points (<50 minutes). However, they have comparable noise levels at later times (Figure 5A). This has been shown by the histogram of the protein levels at t = 10 minutes (Figure 5B). The computed CV value at t=10 minutes is 0.064 for M_3 whereas it is 0.083 for M_4. This difference can be explained by a faster response observed in mechanism M_4, which is consistent with our deterministic simulations. At time points before t = 50 minutes, mechanism M_3 shows gradual change in comparison to mechanism M_4. Due to the sharper changes in mechanism M_4, stochastic simulations predict more variation in this mechanism.

At time points between 50 and 150 minutes, mechanism M_3 shows slightly more variation in comparison to mechanism M_4 (Figure 6B). Since M_4 levels reach to larger mP levels, mechanism M_4 shows less variation between 50 and 150 minutes. In the later time points, these two mechanisms exhibit similar noise structure since both mechanisms approach back to the same steady state levels.

In both cases, the mechanisms that provide the same general behavior (decrease or increase in protein levels) show different noise structures (Figure 6B). Therefore, depending on the needs of the biological system, the cells might selectively employ mechanisms M_1 or M_2. Same is true for mechanisms M_3 or M_4. Interestingly, overall difference between the competing mechanisms are not affected by the initial protein levels when the number of molecules stays smaller than 300 molecules (results are not shown).

======= Figure 4 here ==========

======= Figure 5 here ======================

======= Figure 6 here ======================

3.4 Dependence of the Results on the Protein Abundance

In this section, we explore the effects of protein abundance on the response metrics in all of the mechanisms. The values for the production and degradation parameters were fixed respectively at $\alpha = 10$ and $\beta = 0.02$ in the deterministic analysis of the models above (Figures 2-3). In the stochastic simulations, a small steady state level of 50 molecules/cell in the absence of the signal was selected to investigate effects of noise in the dynamics. As the steady state molecule number increases, the stochastic simulations approach the results of the deterministic simulations(results not shown). To study the effects of the parameters α and β on the response metrics, we utilized the analytic solutions for all the models.

Suppose that $P_1(t)$ is the protein level in mechanism M_1 and $P_2(t)$ is the protein level in mechanism M_2. Then, the dynamics of $P_1(t)$ and $P_2(t)$ are described by the equations in Table 1. The details of the derivation of these solutions are provided in the supplementary materials.

The solutions of our analytical model (Table 1) show that the main results of our study do not depend on the parameters α and β as described below.

Minimum protein abundance (mP): As described in supplementary material the values of $P_1(t)$ and $P_2(t)$ functions at k can be written as $P_1(k) = \frac{\alpha}{(1+\gamma)\beta} + \left(\frac{\alpha}{\beta} - \frac{\alpha}{(1+\gamma)\beta}\right) e^{-\beta(1+\gamma)k}$ and $P_2(k) = \frac{\alpha}{(1+\gamma)\beta} + \left(\frac{\alpha}{\beta} - \frac{\alpha}{(1+\gamma)\beta}\right) e^{-\beta k}$. So, we have $P_1(k) < P_2(k)$ since $e^{-\beta(1+\gamma)k} < e^{-\beta k}$ for any positive k, β and γ. In fact, for any $t \in [0, k]$, $P_1(t) < P_2(t)$ must hold. This observation suggests that mP levels are lower in mechanism M_1 compared to mechanism M_2, and this result does not depend on α and β values.

Minimal response time (mT)**:** Time required to reach minimal $P_1(t)$ and $P_2(t)$ values are theoretically same and equal to k for both models. However, since $e^{-\beta(1+\gamma)t} < e^{-\beta t}$ for any positive t, β and γ, $P_1(t)$ decreases faster than $P_2(t)$. mT is defined as time required to reach for the protein 90% of its minimum value, which makes it shorter for $P_1(t)$. This observation suggests that mT is shorter for mechanism M_1 in comparison to mechanism M_2, and this result is independent from the values of the parameters α and β.

Duration (D)**:** Since the signal is removed from the system at $t = k$ minutes, the same differential equation with different initial conditions describes the dynamics of both $P_1(t)$ and $P_2(t)$ for $t \geq k$. Since $A_1 = P_1(k)$ and $A_2 = P_2(k)$, $A_1 < A_2$ must hold. This leads

to $P_1(t) < P_2(t)$ for all $t > k$. We also know that for any $t \in [0, k]$, $P_1(t) < P_2(t)$ is true, which makes D longer for mechanism M_1. Our numerical simulations confirm this result, and show a slight variation between the two mechanisms.

Integrated Response (IR): Since mP is smaller and D is longer for mechanism M_1, the integrated response IR is larger for this mechanism. Our numerical simulations confirm this result.

The same reasoning is applied to mechanisms M_3 and M_4 using solutions given in Table 1 as detailed in the supplementary materials.

4 Discussions

Understanding dynamics of the cellular regulatory mechanisms is the key for the analysis of cellular functions, disease mechanisms and evolutionary dynamics. Such knowledge is important for finding better diagnoses and therapies for diseases. Mathematical models offer an alternative approach to biological experimentation for studying the regulatory cellular dynamics. In this study, we have compared dynamics of two classes of signal induced regulatory inhibition and activation mechanisms. It is assumed that the signal induced inhibition of proteins can occur in two different ways, either by increasing protein degradation rate or decreasing its production rate. In a similar way, the signal induced activation of proteins can be achieved by decreasing its degradation rate or alternatively increasing its production rate. We developed simple mathematical models to compare and contrast these mechanisms using four different metrics characterizing different aspects of protein dynamics after a time dependent signal has been applied. The metrics used are the highest/lowest protein abundance (mP), the time required for the protein to reach its highest/lowest abundance (mT), the duration of the response (D) and the integrated response (IR). Our analysis shows that the signal-dependent increased degradation mechanism is a quicker, more effective and noisier way of inhibition of the protein compared to the decreased activation mechanism. Furthermore, the signal-dependent increased production mechanism produces a faster and stronger response than the decreased degradation mechanism. We observed that both of the activation mechanisms show similar noise structures although there is a slight difference. Such observations can experimentally be tested using synthetically engineered genetic circuits utilizing fluorescent proteins. Our analysis emphasizes the importance of mathematical modeling in better understanding the dynamics of cellular systems.

Acknowledgment:

We thank Matthew Zaringhalam for his contribution in the literature review in the early stages of this study. We also thank two anonymous referees for their comments and suggestions, which measurably improved this paper. This work was partially supported by the Colgate University Research Council funds and New College of Florida faculty development funds.

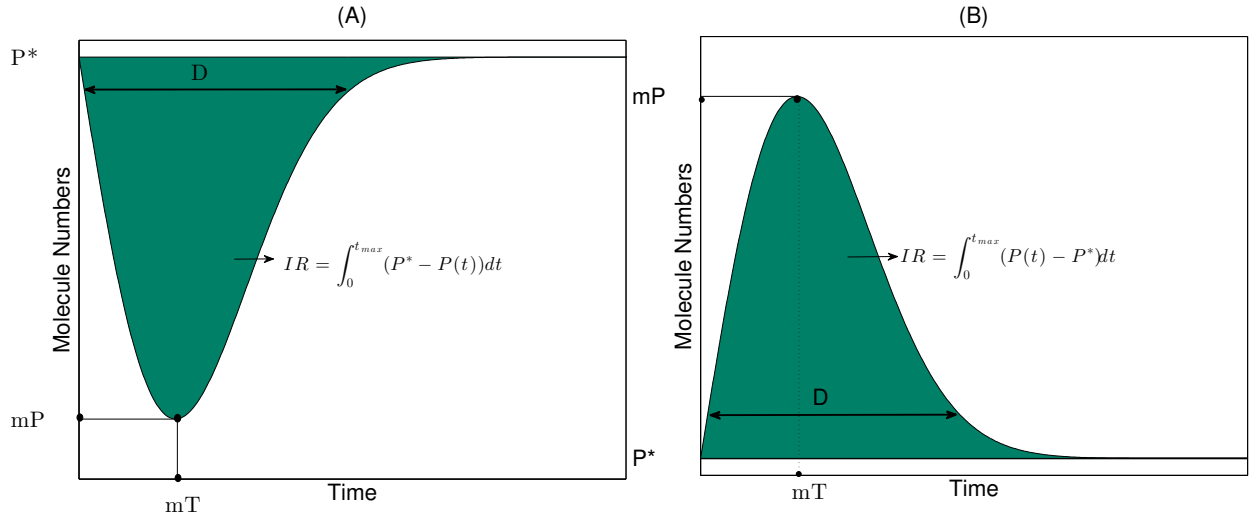

Figure 1: Protein level P for both inhibition (A) and activation (B) mechanisms as a function of time after the system is perturbed by an external signal for a specific period of time. The definitions of the four response metrics that characterize the temporal changes in protein level are minimum/maximum protein abundance (mP), time required for the protein to reach its minimum/maximum level (mT), duration of response (D), and integrated response (IR) are shown.

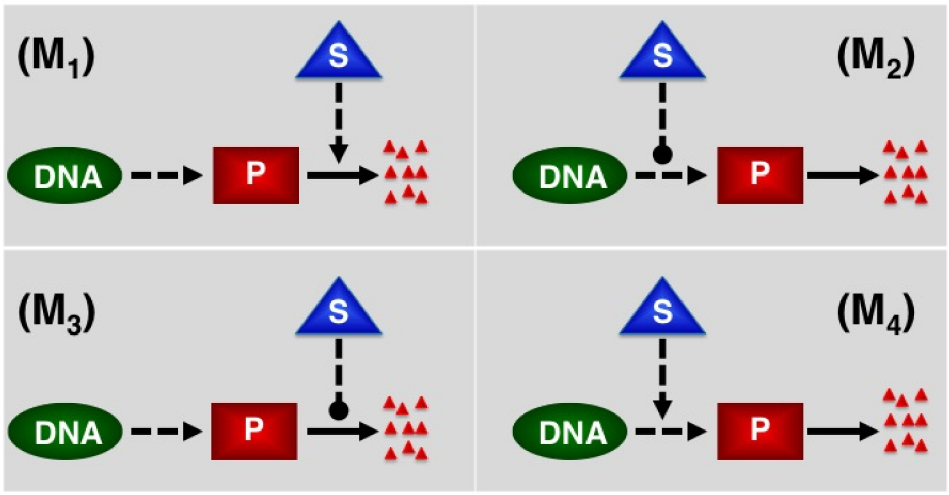

Scheme 1: A cartoon representation of the models for the mechanisms M_1, M_2, M_3 and M_4. The vertical dotted lines with arrows are for signal dependent increase in production or degradations, vertical dotted lines with rounded end shows inhibition in degradation or production. The horizontal solid lines with arrows show degradation of the protein and horizontal dotted lines with arrows show production of the protein.

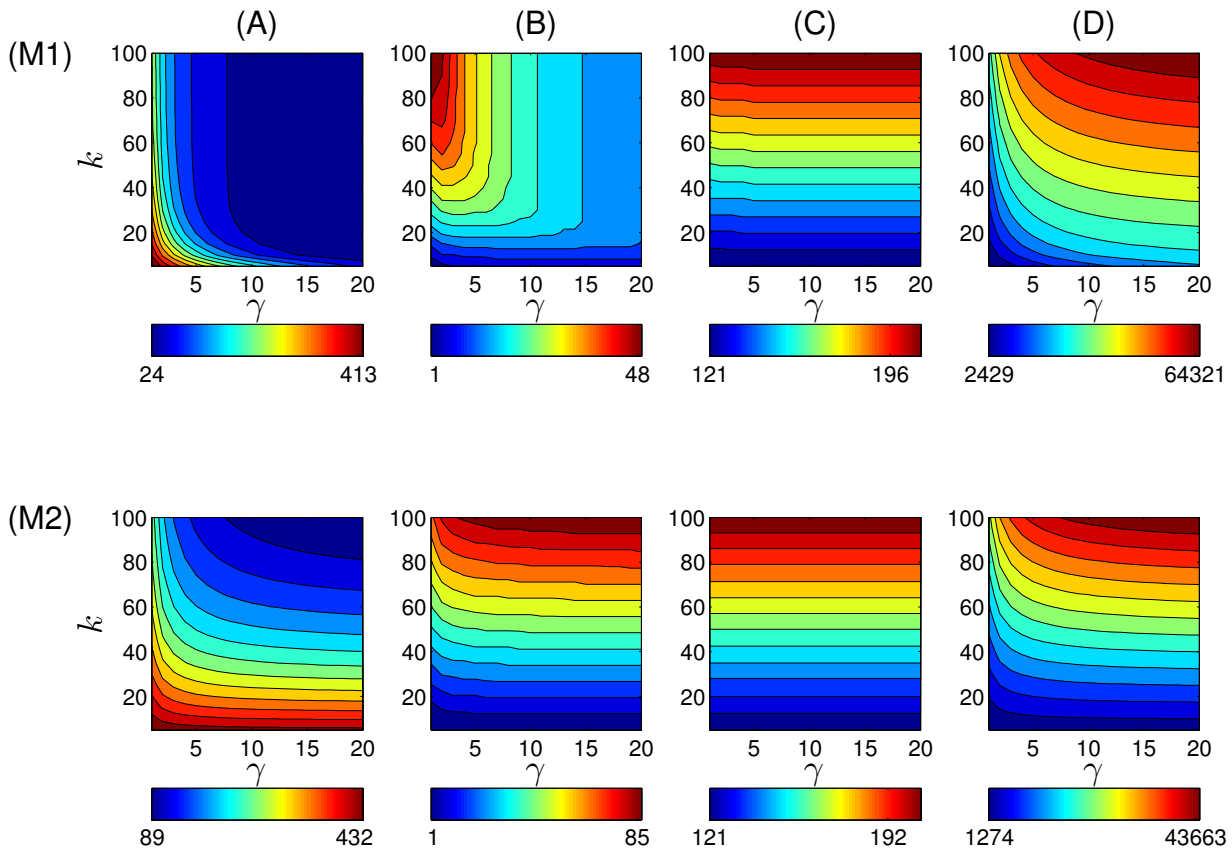

Figure 2: M_1 and M_2 mechanisms' dynamics and characteristics when changing signal with signal amplitude γ ranging from a 1-fold change to a 20-fold change and signal persistency k ranging from 5 to 100 minutes. Increasing the signal intensity results in ∼3.7 fold difference in the minimum protein mP levels between the mechanisms M_1 and M_2 (A). A shorter time is needed to reach minimum protein levels in mechanism M_1 compared to mechanism M_2 (B). No difference on the duration is observed between two mechanisms in response to the differences in the signal (C). The integrated response levels are higher in mechanism M_1 than in mechanism M_2, due to the more severe reductions in minimum protein mP levels in mechanism M_1 (D).

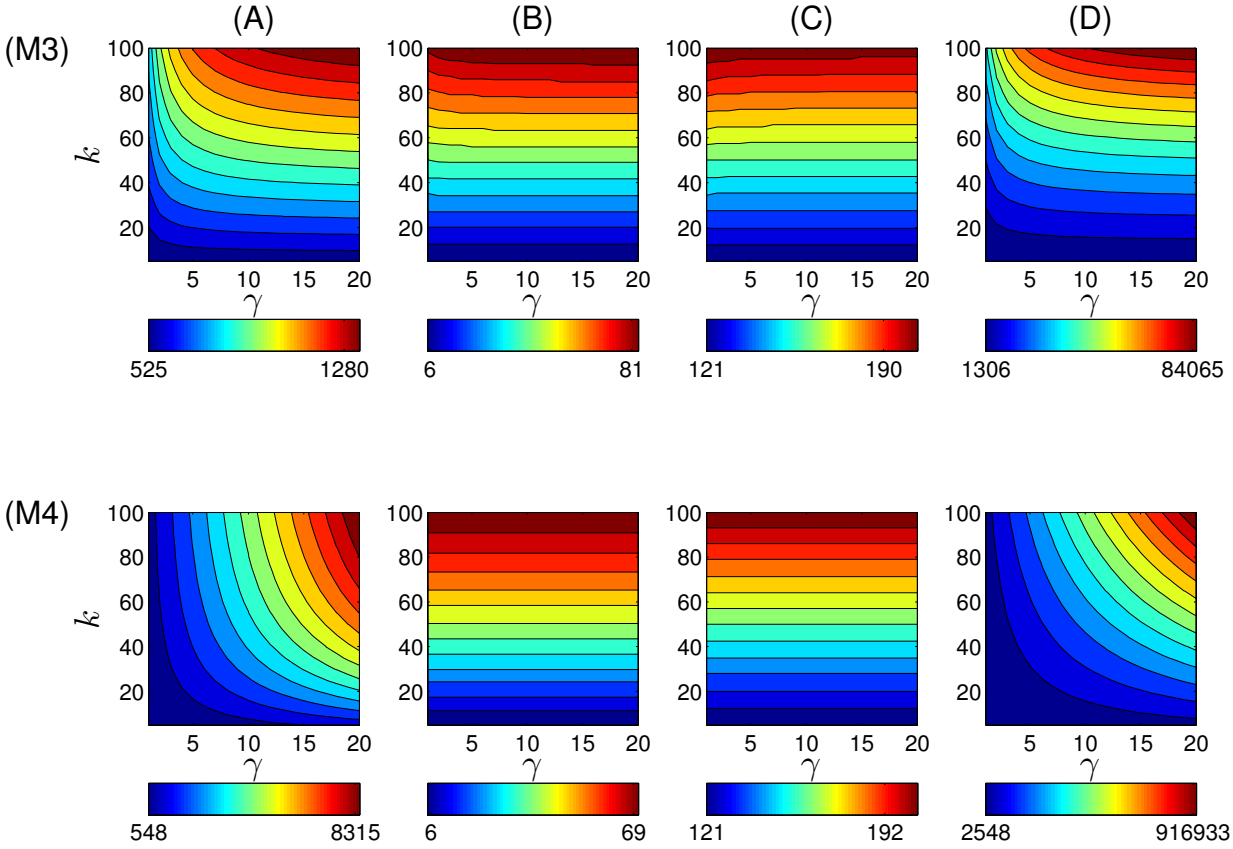

Figure 3: M_3 and M_4 mechanisms' dynamics and characteristics when changing signal amplitude γ from 1 fold to 20 fold, and signal persistency k from 5 to 100 minutes. Increasing the signal intensity results in a $\sim$6.5 fold difference in the maximum protein mP levels between M_3 and M_4 mechanisms (A). Slightly shorter time is needed to reach maximum protein mP levels in mechanism M_4 versus mechanism M_3 (B). No difference on the duration is observed between the two mechanisms in response to the differences in the signal (C). The integrated response levels are higher in mechanism M_4 versus mechanism M_3, due to more severe increase in maximum protein mP levels in mechanism M_4 (D).

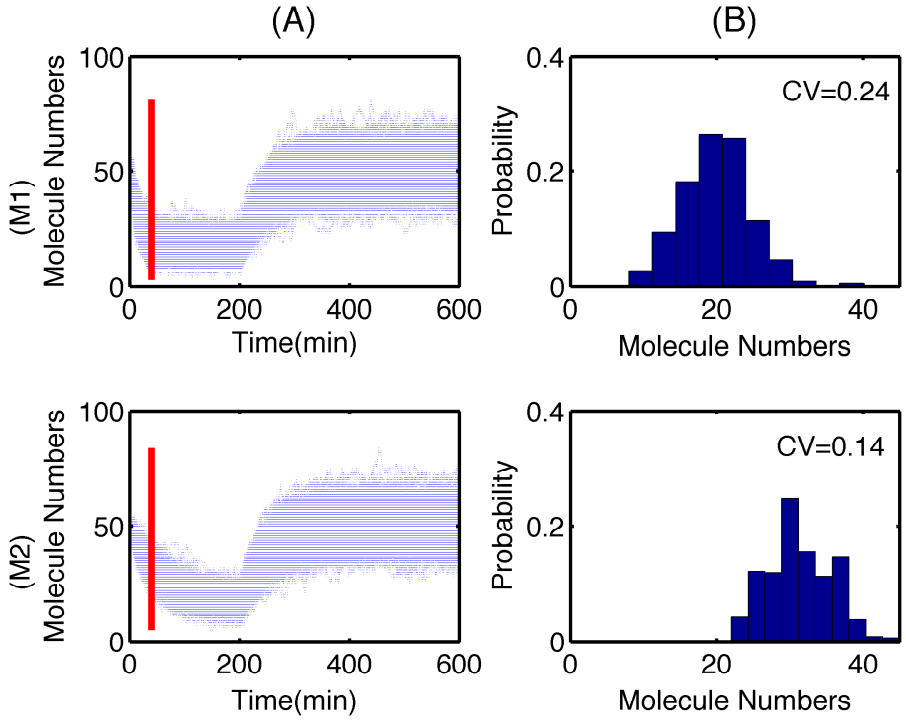

Figure 4: M_1 and M_2 mechanisms' dynamics and characteristics when the number of molecules are low. Five hundred stochastic simulations of the mechanisms M_1 and M_2 are shown on the left (A). Histograms from the stochastic simulations at time 50 min (red lines of the left panel) are shown in the right panel (B). Mechanisms M_1 and M_2 show vastly different noise structures in the early time points just after the signal is applied to the system. Noise levels are measured by using the coefficient of variation (CV) values in 1 minute time intervals.

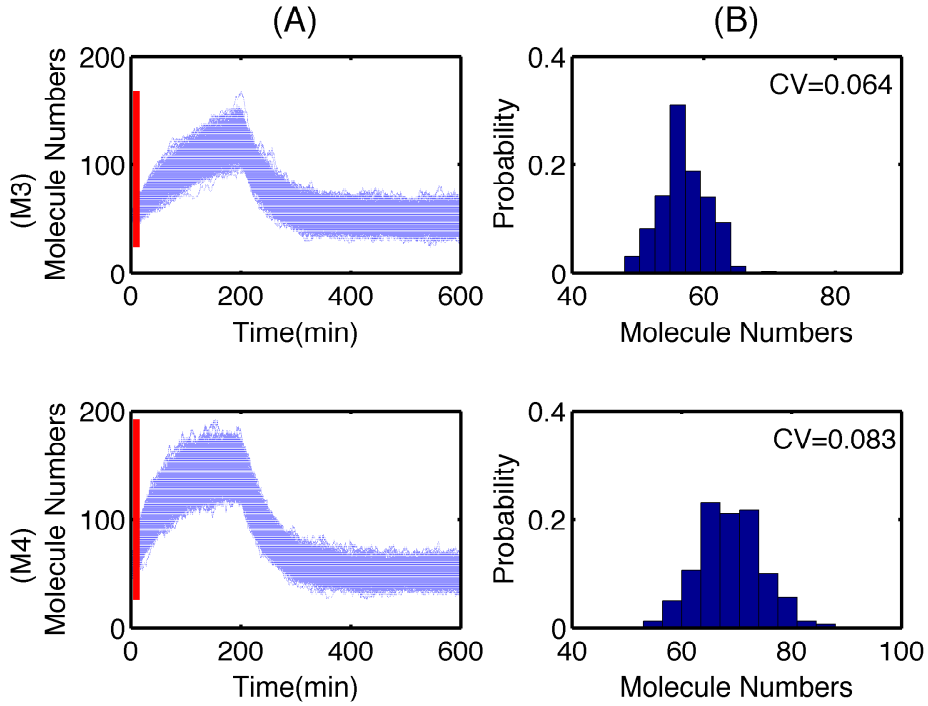

Figure 5: M_3 and M_4 mechanisms' dynamics and characteristics when the number of molecules are low. Five hundred stochastic simulations of the mechanisms M_3 and M_4 are shown on the left (A). Histograms from the stochastic simulations at time 10 min (red lines on the left panel) are shown in the right panel (B). Two mechanisms show slightly different noise structures in the early time points just after the signal is applied to the system. Noise levels are measured by using the coefficient of variation CV values in 1 minute time intervals.

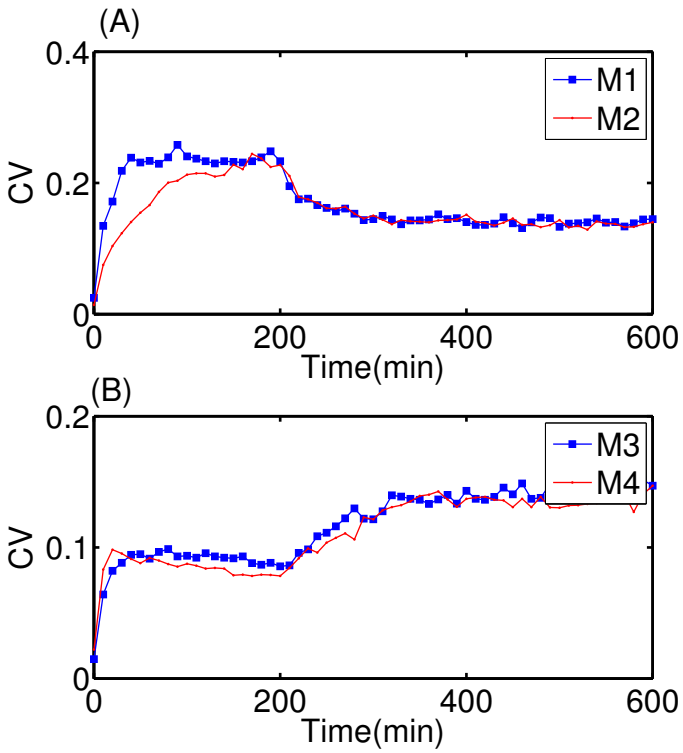

Figure 6: Noise level comparison of the mechanisms throughout the simulation. Mechanisms M_1 and M_2 show different noise levels until approximately 150 minutes (A). M_3 and M_4 mechanisms show slightly different noise levels in early time points, however overall noise structures between these two mechanisms are comparable most of the time (B).

Table 1: The analytical solutions of the models for mechanisms M_j for $j = \{1, 2, 3, 4\}$

$$
\begin{aligned}
M_1\colon\ P_1(t) &= \begin{cases} \frac{\alpha}{(1+\gamma)\beta} + \frac{\alpha}{\beta}\frac{\gamma}{(1+\gamma)}e^{-\beta(1+\gamma)t}, & \text{when} \quad 0 \le t < k \\ \frac{\alpha}{\beta} + \left(A_1 - \frac{\alpha}{\beta}\right)e^{-\beta(t-k)}, & \text{when} \quad t \ge k \end{cases} \\
M_2\colon\ P_2(t) &= \begin{cases} \frac{\alpha}{(1+\gamma)\beta} + \frac{\alpha}{\beta}\frac{\gamma}{(1+\gamma)}e^{-\beta t}, & \text{when } 0 \le t < k \\ \frac{\alpha}{\beta} + \left(A_2 - \frac{\alpha}{\beta}\right)e^{-\beta(t-k)}, & \text{when } t \ge k \end{cases} \\
M_3\colon\ P_3(t) &= \begin{cases} \frac{\alpha(1+\gamma)}{\beta} - \frac{\alpha\gamma}{\beta}\mathrm{e}^{-\frac{\beta t}{1+\gamma}}, & \text{when } 0 \le t < k \\ \frac{\alpha}{\beta} + (A_3 - \frac{\alpha}{\beta})\mathrm{e}^{-\beta(t-k)}, & \text{when } t \ge k \end{cases} \\
M_4\colon\ P_4(t) &= \begin{cases} \frac{\alpha(1+\gamma)}{\beta} - \frac{\alpha\gamma}{\beta}\mathrm{e}^{-\beta t}, & \text{when } 0 \le t < k \\ \frac{\alpha}{\beta} + (A_4 - \frac{\alpha}{\beta})\mathrm{e}^{-\beta(t-k)}, & \text{when } t \ge k \end{cases}
\end{aligned}
$$

References

[1] U. Alon. Network motifs: theory and experimental approaches. *Nat. Rev. Genet.*, 8(6):450–461, Jun 2007.

[2] A. Ay, S. Knierer, A. Sperlea, J. Holland, and E.M. Özbudak. Short-lived her proteins drive robust synchronized oscillations in the zebrafish segmentation clock. *Development*, 140(15):3244–3253, 2013.

[3] I. Braakman and N. J. Bulleid. Protein folding and modification in the mammalian endoplasmic reticulum. *Annu. Rev. Biochem.*, 80:71–99, Jun 2011.

[4] J. A. Brockman, D. C. Scherer, T. A. McKinsey, S. M. Hall, X. Qi, W. Y. Lee, and D. W. Ballard. Coupling of a signal response domain in I kappa B alpha to multiple pathways for NF-kappa B activation. *Mol. Cell. Biol.*, 15(5):2809–2818, May 1995.

[5] T. Cagatay, M. Turcotte, M. B. Elowitz, J. Garcia-Ojalvo, and G. M. Suel. Architecture-dependent noise discriminates functionally analogous differentiation circuits. *Cell*, 139(3):512–522, Oct 2009.

[6] S. D. Catz and J. L. Johnson. Transcriptional regulation of bcl-2 by nuclear factor kappa B and its significance in prostate cancer. *Oncogene*, 20(50):7342–7351, Nov 2001.

[7] J. K. Chun, D. W. Seo, S. H. Ahn, J. H. Park, J. S. You, C. H. Lee, J. C. Lee, Y. K. Kim, and J. W. Han. Suppression of the NF-kappaB signalling pathway by ergolide, sesquiterpene lactone, in HeLa cells. *J. Pharm. Pharmacol.*, 59(4):561–566, Apr 2007.

[8] T. F. Day, X. Guo, L. Garrett-Beal, and Y. Yang. Wnt/beta-catenin signaling in mesenchymal progenitors controls osteoblast and chondrocyte differentiation during vertebrate skeletogenesis. *Dev. Cell*, 8(5):739–750, May 2005.

[9] John Fothergill. *Genes and Signals*. Cold Spring Harbor Laboratory, Cold Spring Harbor, NY, 2002.

[10] F. Gebauer and M. W. Hentze. Molecular mechanisms of translational control. *Nat. Rev. Mol. Cell Biol.*, 5(10):827–835, Oct 2004.

[11] D. T. Gillespie. Exact stochastic simulation of coupled chemical reactions. *J. Phys. Chem.*, 81:2340, 1977.

[12] T. Grimm, S. Schneider, E. Naschberger, J. Huber, E. Guenzi, A. Kieser, P. Reitmeir, T. F. Schulz, C. A. Morris, and M. Sturzl. EBV latent membrane protein-1 protects B cells from apoptosis by inhibition of BAX. *Blood*, 105(8):3263–3269, Apr 2005.

[13] S. Haupt, M. Berger, Z. Goldberg, and Y. Haupt. Apoptosis - the p53 network. *J. Cell. Sci.*, 116(Pt 20):4077–4085, Oct 2003.

[14] Y. Haupt, R. Maya, A. Kazaz, and M. Oren. Mdm2 promotes the rapid degradation of p53. *Nature*, 387(6630):296–299, May 1997.

[15] T. C. He, A. B. Sparks, C. Rago, H. Hermeking, L. Zawel, L. T. da Costa, P. J. Morin, B. Vogelstein, and K. W. Kinzler. Identification of c-MYC as a target of the APC pathway. *Science*, 281(5382):1509–1512, Sep 1998.

[16] T. P. Hill, D. Spater, M. M. Taketo, W. Birchmeier, and C. Hartmann. Canonical Wnt/beta-catenin signaling prevents osteoblasts from differentiating into chondrocytes. *Dev. Cell*, 8(5):727–738, May 2005.

[17] J. S. Ho, W. Ma, D. Y. Mao, and S. Benchimol. p53-Dependent transcriptional repression of c-myc is required for G1 cell cycle arrest. *Mol. Cell. Biol.*, 25(17):7423–7431, Sep 2005.

[18] R. Honda, H. Tanaka, and H. Yasuda. Oncoprotein MDM2 is a ubiquitin ligase E3 for tumor suppressor p53. *FEBS Lett.*, 420(1):25–27, Dec 1997.

[19] S. A. Innocente, J. L. Abrahamson, J. P. Cogswell, and J. M. Lee. p53 regulates a G2 checkpoint through cyclin B1. *Proc. Natl. Acad. Sci. U.S.A.*, 96(5):2147–2152, Mar 1999.

[20] Yasushi Ishihama, Thorsten Schmidt, Juri Rappsilber, Matthias Mann, F Ulrich Hartl, Michael Kerner, and Dmitrij Frishman. Protein abundance profiling of the escherichia coli cytosol. *BMC Genomics*, 9(1):102, 2008.

[21] A. Israel, O. Yano, F. Logeat, M. Kieran, and P. Kourilsky. Two purified factors bind to the same sequence in the enhancer of mouse MHC class I genes: one of them is a positive regulator induced upon differentiation of teratocarcinoma cells. *Nucleic Acids Res.*, 17(13):5245–5257, Jul 1989.

[22] S. M. Kelly and A. H. Corbett. Messenger RNA export from the nucleus: a series of molecular wardrobe changes. *Traffic*, 10(9):1199–1208, Sep 2009.

[23] D. Kimelman and W. Xu. beta-catenin destruction complex: insights and questions from a structural perspective. *Oncogene*, 25(57):7482–7491, Dec 2006.

[24] M. Kollmann, L. Lovdok, K. Bartholome, J. Timmer, and V. Sourjik. Design principles of a bacterial signalling network. *Nature*, 438(7067):504–507, Nov 2005.

[25] R. Kulikov, J. Letienne, M. Kaur, S. R. Grossman, J. Arts, and C. Blattner. Mdm2 facilitates the association of p53 with the proteasome. *Proc. Natl. Acad. Sci. U.S.A.*, 107(22):10038–10043, Jun 2010.

[26] S. H. Lecker, A. L. Goldberg, and W. E. Mitch. Protein degradation by the ubiquitin-proteasome pathway in normal and disease states. *J. Am. Soc. Nephrol.*, 17(7):1807–1819, Jul 2006.

[27] A. J. Levine. p53, the cellular gatekeeper for growth and division. *Cell*, 88(3):323–331, Feb 1997.

[28] M. C. Mackey M. Santillán, E. S. Zeron. *Mathematical Biology Research Trends (ed: Lachlan B. Wilson)*. Nova Science Publishers, Inc., Nova Science Publishers, Inc., 2008.

[29] S. Mangan and U. Alon. Structure and function of the feed-forward loop network motif. *Proc. Natl. Acad. Sci. U.S.A.*, 100(21):11980–11985, Oct 2003.

[30] A. Marette. New insights in covalent modifications of proteins and lipids: phosphorylation and beyond. *Am. J. Physiol. Endocrinol. Metab.*, 296(4):E579–580, Apr 2009.

[31] L. D. Mayo and D. B. Donner. The PTEN, Mdm2, p53 tumor suppressor-oncoprotein network. *Trends Biochem. Sci.*, 27(9):462–467, Sep 2002.

[32] D. Michael and M. Oren. The p53-Mdm2 module and the ubiquitin system. *Semin. Cancer Biol.*, 13(1):49–58, Feb 2003.

[33] U. M. Moll and O. Petrenko. The MDM2-p53 interaction. *Mol. Cancer Res.*, 1(14):1001–1008, Dec 2003.

[34] L. Moore, S. Venkatachalam, H. Vogel, J. C. Watt, C. L. Wu, H. Steinman, S. N. Jones, and L. A. Donehower. Cooperativity of p19ARF, Mdm2, and p53 in murine tumorigenesis. *Oncogene*, 22(49):7831–7837, Oct 2003.

[35] S. Murakami, V. Lefebvre, and B. de Crombrugghe. Potent inhibition of the master chondrogenic factor Sox9 gene by interleukin-1 and tumor necrosis factor-alpha. *J. Biol. Chem.*, 275(5):3687–3692, Feb 2000.

[36] Yildirim N. and Mackey M. C. Feedback regulation in the lactose operon: a mathematical modeling study and comparison with experimental data. *Biophysical Journal*, 84:84, 2003.

[37] A. Oeckinghaus and S. Ghosh. The NF-kappaB family of transcription factors and its regulation. *Cold Spring Harb Perspect Biol*, 1(4):a000034, Oct 2009.

[38] R. Reed. Coupling transcription, splicing and mRNA export. *Curr. Opin. Cell Biol.*, 15(3):326–331, Jun 2003.

[39] K. M. Ryan, A. C. Phillips, and K. H. Vousden. Regulation and function of the p53 tumor suppressor protein. *Curr. Opin. Cell Biol.*, 13(3):332–337, Jun 2001.

[40] O. J. Sansom, K. R. Reed, M. van de Wetering, V. Muncan, D. J. Winton, H. Clevers, and A. R. Clarke. Cyclin D1 is not an immediate target of beta-catenin following Apc loss in the intestine. *J. Biol. Chem.*, 280(31):28463–28467, Aug 2005.

[41] S. S. Shen-Orr, R. Milo, S. Mangan, and U. Alon. Network motifs in the transcriptional regulation network of Escherichia coli. *Nat. Genet.*, 31(1):64–68, May 2002.

[42] O. Shoval and U. Alon. SnapShot: network motifs. *Cell*, 143(2):326–e1, Oct 2010.

[43] M. Shtutman, J. Zhurinsky, I. Simcha, C. Albanese, M. D'Amico, R. Pestell, and A. Ben-Ze'ev. The cyclin D1 gene is a target of the beta-catenin/LEF-1 pathway. *Proc. Natl. Acad. Sci. U.S.A.*, 96(10):5522–5527, May 1999.

[44] N. Sonenberg and A. G. Hinnebusch. Regulation of translation initiation in eukaryotes: mechanisms and biological targets. *Cell*, 136(4):731–745, Feb 2009.

[45] W. Tao and A. J. Levine. P19(ARF) stabilizes p53 by blocking nucleo-cytoplasmic shuttling of Mdm2. *Proc. Natl. Acad. Sci. U.S.A.*, 96(12):6937–6941, Jun 1999.

[46] O. Tetsu and F. McCormick. Beta-catenin regulates expression of cyclin D1 in colon carcinoma cells. *Nature*, 398(6726):422–426, Apr 1999.

[47] B. Vogelstein, D. Lane, and A. J. Levine. Surfing the p53 network. *Nature*, 408(6810):307–310, Nov 2000.

[48] S. D. Westerheide, M. W. Mayo, V. Anest, J. L. Hanson, and A. S. Baldwin. The putative oncoprotein Bcl-3 induces cyclin D1 to stimulate G(1) transition. *Mol. Cell. Biol.*, 21(24):8428–8436, Dec 2001.

[49] P. Wong, S. Gladney, and J. D. Keasling. Mathematical model of the *lac* operon: Inducer exclusion, catabolite repression, and diauxic growth on glucose and lactose. *Biotechnol. Prog.*, 13:132.143, 1997.

[50] Y. Yang, L. Topol, H. Lee, and J. Wu. Wnt5a and Wnt5b exhibit distinct activities in coordinating chondrocyte proliferation and differentiation. *Development*, 130(5):1003–1015, Mar 2003.

[51] F. Yano, F. Kugimiya, S. Ohba, T. Ikeda, H. Chikuda, T. Ogasawara, N. Ogata, T. Takato, K. Nakamura, H. Kawaguchi, and U. I. Chung. The canonical Wnt signaling pathway promotes chondrocyte differentiation in a Sox9-dependent manner. *Biochem. Biophys. Res. Commun.*, 333(4):1300–1308, Aug 2005.

[52] Necmettin Yildirim. Mathematical modeling of the low and high affinity arabinose transport systems in escherichia coli. *Mol. BioSyst.*, 8(4):1319–1324, 2012.

[53] Horike D. Yildirim N., Santillan M. and Mackey M. C. Dynamics and bistability in a reduced model of the lac operon. *Chaos*, 14(2):279–292, 2004.